The Astrophysical Journal Supplement Series, 220:35 (9pp), 2015 October doi:10.1088/0067-0049/220/2/35

IMPACT OF PLANETARY GRAVITATION ON HIGH-PRECISION NEUTRAL ATOM MEASUREMENTS

H. Kucharek[1], A. Galli[2], P. Wurz[2], E. Möbius[1], M. A. Lee[1], J. Park[1], S. A. Fuselier[3,4], M. Bzowski[5], N. A Schwadron[1], and D. McComas[3,4]
[1] University of New Hampshire, 8 College Road, Durham, NH, 03824, USA
[2] Physikalisches Institut der Universität Bern, Bern, Switzerland
[3] Southwest Research Institute, San Antonio, TX, USA
[4] University of Texas at San Antonio, TX, USA
[5] Space Research Centre, Polish Academy of Sciences, Warsaw, Poland
Received 2015 June 24; accepted 2015 July 22; published 2015 October 20

ABSTRACT

Measurements of energetic neutral atoms (ENAs) have been extremely successful in providing very important information on the physical processes inside and outside of our heliosphere. For instance, recent *Interstellar Boundary Explorer* (*IBEX*) observations have provided new insights into the local interstellar environment and improved measurements of the interstellar He temperature, velocity, and direction of the interstellar flow vector. Since particle collisions are rare, and radiation pressure is negligible for these neutrals, gravitational forces mainly determine the trajectories of neutral He atoms. Depending on the distance of an ENA to the source of a gravitational field and its relative speed and direction, this can result in significant deflection and acceleration. In this paper, we investigate the impact of the gravitational effects of Earth, the Moon, and Jupiter on ENA measurements performed in Earth's orbit. The results show that current analysis of the interstellar neutral parameters by *IBEX* is not significantly affected by planetary gravitational effects. We further studied the possibility of whether or not the Helium focusing cone of the Sun and Jupiter could be measured by *IBEX* and whether or not these cones could be used as an independent measure of the temperature of interstellar Helium.

Key words: gravitation – ISM: atoms

1. INTRODUCTION

Measurements using neutral atoms have tremendously enhanced the opportunities for exploring the local interstellar environment. For instance, *Ulysses* provided the first measurement of the interstellar neutral (ISN) Helium (He) gas flow at distances ranging from 1.3 to 3 AU from the Sun using a neutral particle instrument (Witte et al. 1992). From these measurements, the speed, temperature, and direction of the interstellar He flow were determined with the help of an (ISN) trajectory model. These measurements addressed only interstellar neutral He gas. The *Interstellar Boundary Explorer* (*IBEX*; McComas et al. 2009) spacecraft, launched in 2008, uses two highly sensitive neutral atom cameras on a Sun-pointing spinning spacecraft and scans the entire sky with a half-year cadence. For more details concerning the *IBEX* instruments and their measurement capabilities, we refer the reader to the respective *IBEX* instrument papers (Funsten et al. 2009; Fuselier et al. 2009).

The interstellar medium consists of charged particles, dust, and neutral atoms. The charged particles are tied to the interstellar magnetic field lines and do not enter the heliosphere. Neutral atoms, however, can enter the heliosphere, and if they are not ionized (e.g., by solar UV radiation or charge exchange with the solar wind) or deflected by solar radiation pressure, they can reach Earth's orbit and *IBEX* can measure them. This population of neutral atoms is called the direct ISN flow. If a neutral particle approaches the gravitational potential of a planet, a moon, or the Sun it will follow Keplerian/hyperbolic orbits.

In our solar system, the Sun, due to its mass, generates the strongest gravitational field. The strength of the gravitational forces acting on a particle trajectory depends on the distance between a massive particle and another massive object. A known effect of the Sun's gravitational force on the trajectories of neutral particles is the gravitational focusing cone (Möbius et al. 1985, 1995). The Sun's gravitation focuses interstellar neutral He atoms downwind of the Sun into a cone-shaped density enhancement. Earth passes through this cone-like structure in December every year. This feature has been investigated with several space probes including the *Solar and Heliospheric Observatory*, using UV scattering (Michels et al. 2002), and *STEREO*, using pick-up ions (Saul et al. 2009; Drews et al. 2010). In addition to the Sun's gravitational forces, neutral atoms are also exposed to radiation pressure and ionization. These interactions are particularly important for neutral measurements in Earth's orbit because ionization by solar radiation can significantly reduce the number of neutral atoms and radiation pressure can deflect the neutral atoms. In particular, hydrogen is heavily depleted with respect to ISN helium due to this effect. Gravitational forces depend only on the mass of the objects and the relative distance between the neutral atom and the gravitational source. The gravitational force of the planet can surpass the gravitational force of the Sun when the neutral atom is close enough to the planet.

Compared to the *Ulysses* spacecraft (Witte et al. 1992), which took neutral measurements at a distance of 1.3–3 AU, which is far from planets or moons, *IBEX* performs energetic neutral atom (ENA) measurements in Earth's orbit, and changes in deflection angles due to Earth's gravity may be important. These neutral atoms are traveling at high speeds, and therefore it is expected that these angular changes may be small. However, the determination of the ISN parameters strongly depends on the accuracy of the interstellar flow direction. A change of even just one degree can have a significant impact on the determined speed and the temperature of the interstellar flow (see McComas et al. 2012; Möbius et al. 2015) for the equations that show the strong coupling of interstellar parameters allowable by *IBEX* observations. Therefore, the goal of this paper is to investigate the possible impact of Earth's gravitation on the *IBEX* measurements.

The purpose of this study is to investigate all of the possible gravitational effects that could impact current and future neutral atom measurements with a spacecraft in Earth's orbit such as *IBEX*. This paper contributes to the error and uncertainty estimates of the interstellar flow parameters derived from *IBEX* measurements. This paper is organized as follows. In Section 2, we address the basic theory for the trajectory of an atom in the vicinity of a gravitational field and the associated acceleration. In Section 3, we investigate the possible impact of the Earth's gravitation on deflection of the interstellar ENAs during the fall and spring seasons. In Section 4, we discuss the impact of the Earth's gravitation on the measured fall signal. We will also discuss the impact of the gravitational forces of the Moon and Jupiter on neutral atom measurements. Before we summarize, we will also discuss the possibility of detecting the gravitational focusing cones.

This study is part of a coordinated set of papers on interstellar neutrals as measured by *IBEX*. The paper by McComas et al. (2015) provides an overview of this *Astrophysical Journal Supplement Series* Special Issue.

2. NEUTRAL MEASUREMENTS NEAR A PLANET OR A MOON

The trajectory of an interstellar neutral atom in the gravitational field of a planet orbiting the Sun is a three-body problem. Depending on the distance between the planet and the atom, the contribution of the forces acting on the atom is mostly determined by the gravitational field of the Sun or the planet, or a combination of both. In our solar system, the Sun—because of its mass—has the largest gravitational potential. However, if the distance of an atom to a planet is sufficiently small or the planetary gravitational field is sufficiently large, then the atom will experience the same or more attraction from the planet than from the Sun. At some distance from the planet, the atom moves on a trajectory without (or with little) an effect from the Sun's gravitation. Under these circumstances, the three- or even many-body problem (if moon(s) are orbiting the planet) can be reduced to a two-body (planet-atom) problem. The distance at which an atom is mostly under the gravitational influence of a planet is well known through celestial mechanics. In three dimensions this is the radius of a sphere, which is called the sphere of influence (SI), with a radius of

$$r_{\mathrm{SI}} = R_{\mathrm{SP}} \left(\frac{M_{\mathrm{P}}}{M_{\mathrm{Sun}}} \right)^{2/5}, \tag{1}$$

where R_{SP} is the distance between the Sun and the planet, M_{p} is the mass of the planet, and M_{Sun} is the mass of the Sun. In the case of Earth, the sphere of influence is 145 Earth radii (R_{E}), or 2.4 times the distance between Earth and the Moon. For this study, we will concentrate on a two-body problem. For the validity of this approach, we refer interested readers to Fahr et al. (1976).

IBEX is orbiting Earth in a highly elliptical orbit (with an apogee altitude of $\sim 50_{\mathrm{RE}}$ and a perigee altitude between 5000 and 12,000 km). Following a maneuver in 2011, the *IBEX* spacecraft was injected into a new, more stable orbit with a perigee of $\sim 8\ R_{\mathrm{E}}$. For more information, see McComas et al. (2011). Figure 1 shows a sketch of a typical pre-maneuver orbit of *IBEX* when taking measurements of interstellar atoms in the spring (left) and fall (right) of each year. To minimize magnetospheric contamination of the interstellar neutral measurements, the *IBEX* data recording starts and ends when the spacecraft is at a distance of $\sim 15\ R_{\mathrm{E}}$ from Earth. The Moon orbits the Earth at an average distance of about 60 R_{E} and the distance to the *IBEX* spacecraft varies. Compared to Earth, it has a much lower mass (0.012 Earth's masses), and thus its gravitational acceleration is smaller, as is its sphere of influence ($r_{\mathrm{Moon}}/r_{\mathrm{Earth}} < 1/13$).

As mentioned above, within the sphere of influence, any neutral particle is mainly in the gravitational field of the Sun, a planet, or a moon. Depending on the energy of the neutral particle and the relative orientation of the velocity vectors of the particle and the planet, the particle may either gain or lose energy and speed and will change direction. This effect is well known in orbital mechanics as gravity assist or gravitational deflection (see van Allen 2002 for a tutorial).

2.1. Gravity Assist on ENAs

If particles are within the sphere of influence of a planet or a moon, then the gravitational fields will change the magnitude and direction of the velocity vector of these particles. The mass of the planet and the particle will not change, and the total momentum is conserved.

$$D V_{\infty} = r_{\mathrm{p}} V_{\mathrm{P}}. \tag{2}$$

In Equation (2), D is the impact parameter (the distance from the asymptote of a hyperbolic trajectory to the center of mass of the planet). Vp is the velocity of the particle at the pericenter radius r_{p} (the radial distance of the closest approach to the planet). Using energy conservation, we obtain

$$r_P = -\frac{G_{\mathrm{pl}}}{V_{\infty}^2} + \sqrt{\frac{G_{\mathrm{pl}}^2}{V_{\infty}^4} + D^2}. \tag{3}$$

In this simple picture, we also assume that the energy of the particle is conserved in the reference frame of the planet but not in the direction of the velocity. For a neutral atom that enters the sphere of influence from infinity on a hyperbolic trajectory to the center of mass with a velocity of V_{∞}, one can determine the asymptotic bending angle α (Cornelisse et al. 1979) see

$$\sin\left(\frac{\alpha}{2}\right) = \frac{1}{1 + \dfrac{r_{\mathrm{p}} V_{\infty}^2}{G_{\mathrm{pl}}}} = \frac{1}{\sqrt{1 + \dfrac{D^2 V_{\infty}^4}{G_{\mathrm{pl}}^2}}}, \tag{4}$$

where G_{pl} is the gravitational parameter of the planet, $G_{\mathrm{pl}} = M_{\mathrm{p}}\ G$. Here, M_{p} is the planet mass and G is the universal gravitational constant. Figure 2 illustrates the situation and explains all of the geometric parameters used in Equations (2)–(4). Note that the deflection angle is independent of the masses of the neutral particles.

This is a very simplistic approach with a number of restrictions. In this approach, we calculate the deflection in the plane of the trajectory around a planet and the problem is reduced to two dimensions. Also, atmospheric effects (which play a role for very close flybys of planets with dense atmospheres) are not included. As Equation (4) shows, the deflection angle in this simple, planetocentric model only depends on the impact parameter and the velocity of a particle.

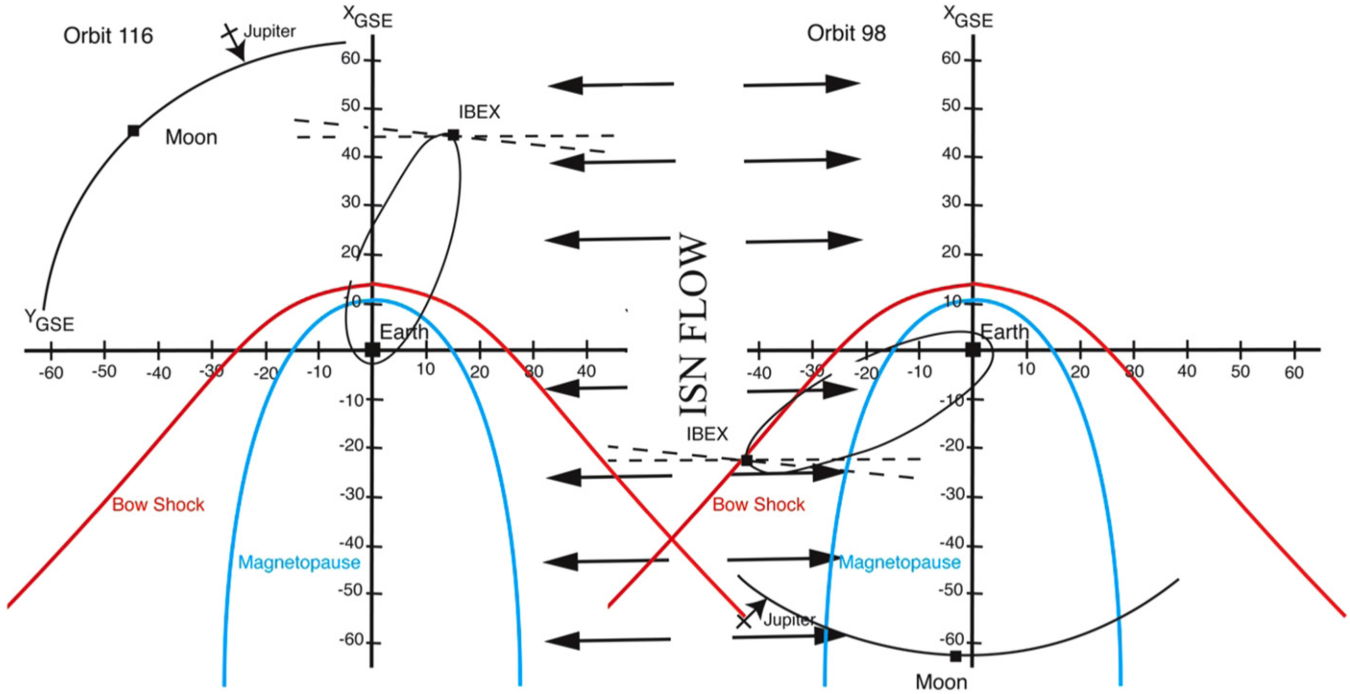

Figure 1. (Right) Orbit# 98 a typical fall orbit and (left) orbit# 116 a typical spring orbit of the *IBEX* spacecraft. The dashed lines show the *IBEX* field of view (FOV). Also shown is the Moon's orbit (black line), Earth's bow shock (red line), and the magnetopause (blue line). The thick black arrows indicate the INS flow, whereas the thin black arrow indicates the direction from Jupiter.

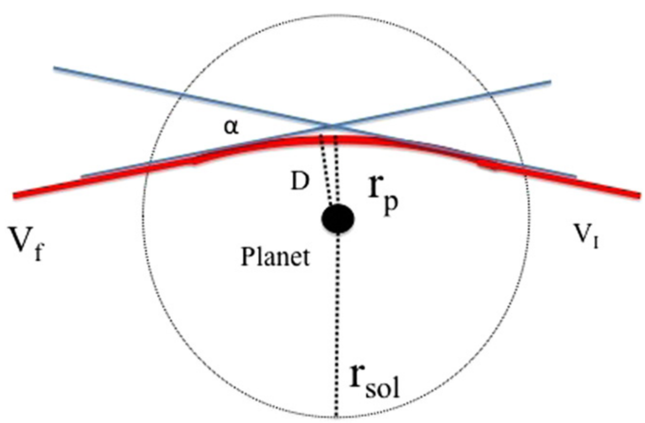

Figure 2. Gravity assist near a planet. The parameter D is the impact parameter. The pericenter radius is denoted by r_p. The angle α is the bending angle.

This deflection angle is extremely important because all of the determined parameters of the interstellar flow, such as the bulk velocity of the flow and the temperature, depend on the accuracy of this angle. We now investigate the possible impact of Earth's gravitational field on *IBEX* measurements during the spring and fall seasons by measuring the interstellar flow and determining the interstellar flow parameters.

3. INTERSTELLAR NEUTRAL FLOW MEASUREMENT

The determination of the physical parameters of the interstellar flow beyond the termination shock is a difficult endeavor because it is very sensitive to the measured direction which the ISN flow arrives at *IBEX*. This flow direction (determined by two angles) is very closely coupled to the bulk speed and the temperature of the interstellar flow at infinity/(in interstellar space; Bzwoski et al. 2012; McComas et al. 2012; Möbius et al. 2012, 2015; Bzowski et al. 2015; Leonard et al. 2015; Schwadron et al. 2015). For hydrogen, understanding the integrated effects of the radiation pressure of the Sun is also critical for resolving the inflow parameters of this species (Schwadron et al. 2013). There are two seasons during which *IBEX* could, in principle, observe the interstellar flow: in spring (February and March) and fall (October and November) of each year where the peak of the ISN signal is observed. In spring, *IBEX*, in its orbit of Earth, is moving into the ISN flow, while in fall *IBEX* is moving along with the flow. Figure 3 shows various positions in the *IBEX* orbit, *IBEX*'s field of view (FOV), and the orientation of the Earth's bow shock (blue line) and the magnetosphere during the spring (lower part) and fall seasons (top part), respectively.

As shown in Figure 3, during the spring season, the spacecraft orbit is mostly outside of the magnetosphere and it is possible to detect ENAs in the pristine solar wind. The impact from Earth's bow shock is very limited. This clear viewing time was actually one of the design constraints for the original *IBEX* mission. This design drove the launch window to guarantee the first six months of global ENA viewing and the ram-direction ISN season (the spring season). During the fall seasons, the spacecraft orbit is mostly inside the magnetosphere or downstream of Earth's bow shock. Only at the end of the fall season can the spacecraft observe ENAs outside of the bow shock. Therefore, the fall ENA observations are performed in an environment of enhanced background level, which needs to be considered in the data analysis (Galli et al. 2015). An enormous advantage is the triple coincident technique, which is built into the *IBEX*-lo detector and guarantees low noise and background levels (Funsten et al. 2009; Fuselier et al. 2009; Wurz et al. 2009).

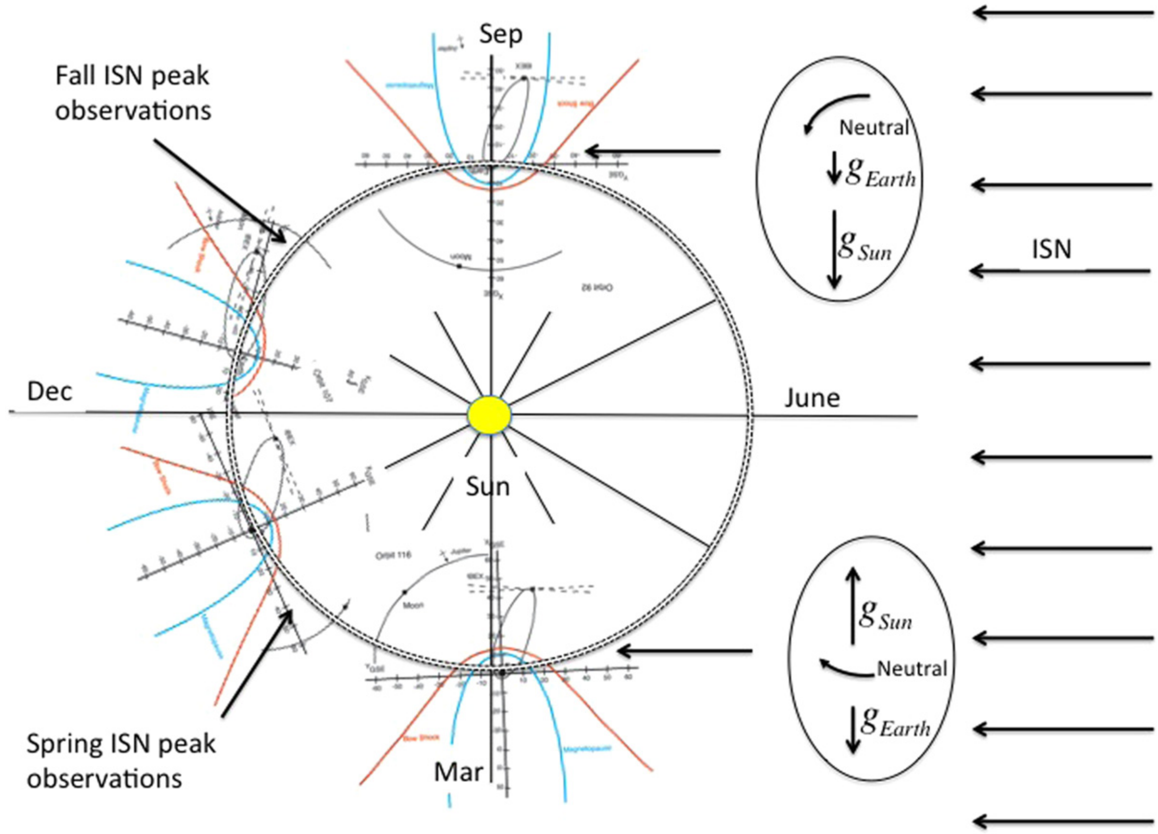

Figure 3. *IBEX* orbits during the spring (January–March) and fall (September–November) seasons. Shown is the flow direction of the interstellar neutrals, the orientation of the magnetopause and Earth's bow shock with respect to the Sun, and the orientation of the *IBEX* orbit and the FOV. This figure also shows the gravitational deflection by Earth relative to the Sun in fall and spring.

In this paper, however, we will concentrate on gravitational effects only. The biggest gravitational effect is from the Sun. The sphere of impact of the Earth is small compared to the sphere of influence of the Sun, and therefore the gravitational impact of the Sun on the large scale is larger than the impact of Earth's. Thus, gravitational effects from Earth are considered to constitute a relatively small contribution. The bending angle only depends on the strength of the gravitational force (distance to the planet) and on the time a particle stays in the sphere of impact, that is, the speed of the particle. In the fall season, the spacecraft orbit is outside of Earth's orbit. *IBEX* starts collecting ENAs at a radial distance from Earth at 15 R_E. Therefore, the ISN flow is collected outside of Earth's orbit and the gravitational acceleration of the Sun and the Earth add up and produce a slightly larger deflection of the neutral flow. During the spring season, the ISN flow would be detected inside Earth's orbit where the gravitational forces act on the neutral particles and try to move them in opposite directions. Then, the bending angle is slightly smaller than without Earth's gravity. For a particle of a given speed, the bending angle is the same in fall and in spring. The biggest difference between the spring and fall seasons is the arrival velocity of the ENAs with respect to Earth. During the spring season, the speed of the ISN flow as seen by *IBEX* is higher than during fall because Earth is moving against the ISN flow. In the following, we determine the average deflection angle as a function of the ISN bulk flow speed. Although possible, but relatively complicated, an exact description of the deflection angle during every orbit is outside the scope of this paper.

3.1. ISN Spring Season

During the ISN spring season, *IBEX* orbiting the Sun is moving toward the interstellar flow. The bulk velocity of the interstellar neutrals is then the sum of the Sun's motion with respect to the interstellar medium plus Earth's motion with respect to the Sun plus the velocity the neutral atoms gained due to the Sun's gravitational acceleration. As described above, the correctness of the inferred ISN parameters depends crucially on all of the gravitational forces, which when combined determine the peak location of the distribution.

Using Equation (4), we determine the possible impact of Earth's gravitational field. We use the distance of the closest approach r_P and the velocity of the atom at infinity and calculate the deflection angle α. Figure 4 shows a contour plot of the deflection angle α as a function of r_P and the speed of the atom. The deflection angle becomes larger with decreasing distance to the planet and decreasing particle velocity.

Figure 3 illustrates that in fall the gravitational force of the Earth adds to the gravitational force of the Sun, whereas in spring it acts against it. The deflection of the ENA trajectories is significantly larger in fall than in spring because of the slower speed of the ISN with respect to Earth's orbital speed. During the spring season, the population of interstellar neutral helium atoms has a bulk velocity of 80 km s^{-1}, which corresponds to 132eV.

The shaded areas in Figure 4 mark the velocity ranges of an interstellar neutral atom for the fall and spring seasons, respectively. The contour lines indicate the range of deflection angles at different distances r_P (in units of Earth radius R_E) of

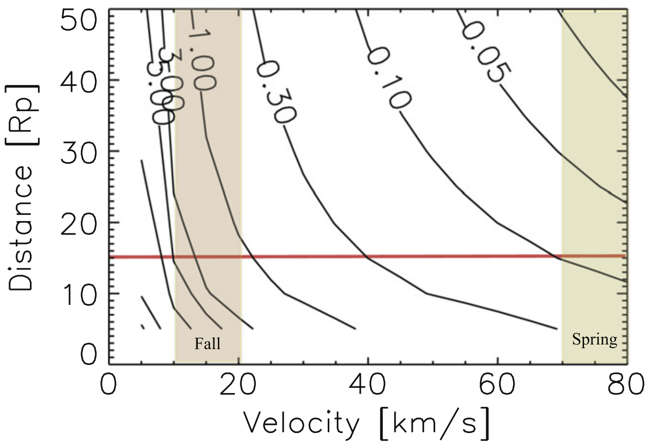

Figure 4. Deflection angle as a function of ENA velocity and distance of the closest approach r_P. The contour lines show the deflection angle α in degrees. The areas shaded in light brown and light green show the angular range/velocity range of the ENAs in fall and in spring, respectively. The red line indicates the distance at which *IBEX*-Lo starts/stops detecting science data.

nearest approach. As one can see, the maximum deflection angle above the red line marking the 15 R_E limit ranges from $\alpha = 5°$ to $\alpha = 0\overset{\circ}{.}01$. The most likely deflection angle for an atom with a velocity of $V = 75$–$80\,\mathrm{km\,s^{-1}}$ at a distance of $r_P = 15\,R_E - 50\,R_E$ is in the range $\alpha = 0\overset{\circ}{.}1$–$0\overset{\circ}{.}03$ degrees in the spring season. These additional deflection angles are quite small and the impact on the deduced ISN flow speed, flow vector, and temperature will be very small.

3.2. ISN Fall Season

In fall *IBEX* orbits Earth and is moving with the interstellar flow, and therefore the bulk speed of the atoms with respect to Earth and *IBEX* is lower and so is the energy of a neutral entering the instrument. A relative velocity between *IBEX* and the interstellar neutrals of 10–20 $\mathrm{km\,s^{-1}}$ corresponds to a peak energy of the ISN distribution of 2–8 eV for helium. This peak energy is lower than the lowest energy step of *IBEX*-Lo, 11–21 eV. Therefore, during the first fall season in 2009, *IBEX*-Lo did not detect a clear signal of the interstellar flow. For the fall season in 2010, a new operational mode was employed which allowed the detection of neutral atoms with bulk energies of 7–15 eV. As pointed out in the paper by Galli et al. (2015), the energy of the He neutrals is below the sputtering threshold at these energies, and thus is not observable by *IBEX*. These authors also showed that the Fall oxygen signal is of the order of one count/hour, which is approximately the same count rate as the background generated by the energetic ions of Earth's magnetosphere. Therefore, it is even more important to provide a theoretical prediction of the peak location of the ISN flow. Because of the lower bulk speed, neutral atoms entering the sphere of influence of a planet are exposed longer to the gravitational field. This leads to a larger deflection angle α.

Figure 4 also shows the situation during the fall season (see brown shaded area). For neutral atoms within a velocity range of 15–20 $\mathrm{km\,s^{-1}}$ and a distance r_p larger than 15 R_E, one would expect a deflection angle in the range of $0\overset{\circ}{.}4$–$5°$. Compared to the spring season, this is a significant change in the arrival direction, which needs to be added to the deflection due to the Sun's gravity. While for the spring season the impact of the Earth's gravity might be negligible, or in the range of other systematical errors, it would have a much larger effect on the results for the interstellar parameters, such as flow speed and temperature, in the fall season.

3.3. Impact on the Velocity and Temperature Determination

Any additional change to the bending angle may result in an uncertainty of the determination of the peak location in the ecliptic longitude of the interstellar neutral atoms as well as on the width of the distribution angle. Furthermore, during any orbit *IBEX* is collecting neutrals at different distances from Earth and at different locations along Earth's orbit. To address this problem in a fully self-consistent manner would require extensive numerical simulations, which is beyond the scope of this paper. Here, we estimate the minimum and maximum impacts of Earth's gravity on the velocity and the temperature of the interstellar flow. In the *IBEX* analysis of the interstellar parameters, these are not independent, they are correlated. In the following, we study the correlated uncertainty of the velocity and temperature of the interstellar flow.

In the *IBEX* data analysis, these two parameters (location and width of the distribution) determine the bulk speed of the interstellar flow into the heliosphere as well as the temperature of the interstellar neutral in interstellar space. The velocity and temperature determination have been described in previous publications (McComas et al. 2012; Möbius et al. 2012; Lee et al. 2012). Using their approach, one obtains a direct relation between the change in the angle in ecliptic longitude at infinity λ_{ISM} and the change of the speed of the interstellar flow V_{ISM}.

Under the assumption that λ_{peak} is accurate, one has a relation between $\Delta\lambda_{\mathrm{ISM}}$ and ΔV_{ISM}

$$\Delta\lambda_{\mathrm{peak}} = \lambda_{\mathrm{peak}} + \alpha = \cos^{-1}\left(-1\middle/\left(1 + \frac{\Delta V_{\mathrm{ISM}}^2}{V_E^2}\right)\right), \quad (5)$$

where α is the angular change due to the Earth's gravitation. For the change in V_{ISM}, we obtain

$$\Delta V_{\mathrm{ISM}} = V_{\mathrm{ISM}} + V_\alpha = V_E\sqrt{\frac{-1}{\cos\left(A + \Delta\lambda_{\mathrm{peak}}\right)} - 1}\,. \quad (6)$$

In this equation, V_α is the variation in velocity infered from the change in angle in ecliptic longitude due to the Earth's graviation. The constant $A = 180 - \lambda_{\mathrm{peak}}$. In most of the recent papers on *IBEX* observations of the interstellar flow, the temperature of the interstellar medium is defined using the Mach number M_A, which is the ratio of V_{ISM}/C_S, where C_S is the speed of sound. If the gas is adiabatic, then the speed of sound is given by

$$C_s^2 = \gamma\frac{P}{\rho}, \quad (7)$$

where γ is the adiabatic index for an ideal gas. For an atomic gas $\gamma = 5/3$. For diatomic molecular gases (such as for molecular hydrogen gas in cold interstellar clouds (H_2)) $\gamma = 7/5$. The pressure P links the temperature and the number density N:

$$P = Nk_BT, \quad (8)$$

Table 1
Change of the Inflow Longitude, the Inflow Velocity, and the Temperature of the Interstellar Flow Due to Earth's Gravitational Effects

Season	$\Delta\ \lambda_{\mathrm{ISM}}$ (deg)	$\Delta\ V_{\mathrm{ISM}}$ (km s^{-1})	$\Delta\ V_{\mathrm{ISM}}/V_{\mathrm{ISM}}$	$\Delta\ T$(K)	$\Delta T/T_{\mathrm{ISM}}$
Spring	0–0.1	0–0.066	0.275%	0–48	0.57%
Fall	0.4–5.0	0.33–3.6	15%	273–2910	34.6%

Note. Note that for the relative values, we used the maximum ΔV and ΔT.

where k_{B} is the Boltzmann constant. Under these assumptions, for the temperature we obtain

$$T = \frac{P}{Nk_{\mathrm{B}}} = \frac{C_s^2 \rho}{Nk_{\mathrm{B}}\gamma} = \frac{V_{\mathrm{ISM}}^2 N_{\mathrm{A}}}{M^2 \gamma k_{\mathrm{B}}}, \tag{9}$$

where N_{A} is the atomic mass of the gas and M is the Mach number. Note that V_{ISM} and M are a function of λ, as is T.

In this approach, the impact of an interstellar magnetic field or an additional hotter or colder interstellar gas component have not been taken into account for the ISN particle distributions. Both would change the Mach number. For instance, a significant contribution of the so-called "Warm Breeze" (Kubiak et al. 2014) could change the Mach number. Following the arguments described in McComas et al. (2012), for the Mach number we find

$$M^2 = a_0 + a_1 \lambda_{\mathrm{ISM}}, \tag{10}$$

where a_0 and a_1 are the fit parameters. The temperature is now a function of λ_{ISM} and V_{ISM}, which also depends on λ_{ISM}. For the temperature change, we obtain

$$\Delta T = \frac{N_{\mathrm{A}}}{\gamma k_{\mathrm{B}}} \frac{\Delta V_{\mathrm{ISM}}^2}{\left(a_0 + a_1 \Delta\lambda_{\mathrm{ISM}}\right)}. \tag{11}$$

Using Equations (9) and (14), we can determine the velocity change as well as the temperature change, which is due to Earth's gravitation. As stated previously, we assume that the biggest gravitational effects are due to the Sun's gravity, and the effects of Earth's gravity are treated as relatively small perturbations. We therefore use the constants a_0 and a_1 and the λ_{peak} (which is measured) from the paper by McComas et al. (2012; Möbius et al. 2012) and determined ΔV_{ISM} and ΔT, with $a_0 = -13.5$, $a_1 = 0^\circ\!.489$, and $\lambda_{\mathrm{Peak}} = 130.29 \pm 0^\circ\!.47$. In Table 1, we summarize the results for the velocity and temperature changes during fall and spring due to Earth's gravitation. For more detailed information on the error estimation on the width of the distribution, we refer interested readers to Möbius et al. (2015).

4. DISCUSSION

As described above, the derivation of the interstellar parameters from the *IBEX*-Lo measurements are model dependent. Because of the numerical complexity, all of the current models do not include effects due to Earth's gravity. This analysis shows that the gravitational effects of Earth have relatively negligible effects on the measurements taken during the spring season, but could have significant impact in the fall if *IBEX* were able to make measurements then. The deflection during the spring season appears to be small ($\alpha = 0^\circ\!.1$–$0^\circ\!.03$). ENAs around 15 R_{E} would experience a deflection of $\alpha = 0^\circ\!.1$ and at 50 R_{E} a deflection of $\alpha = 0^\circ\!.03$, respectively. When passing Earth's sphere of influence, the ISN flow distribution may also be slightly focused by gravitational deflection (Möbius et al. 2015). In fall, this deflection may also lead to a broadening effect of the distribution function, which can lead to a higher apparent temperature.

If we were able to make measurements, or if a future detector on a future mission would be able to take fall measurements, then one would have to take the following considerations into account.

In fall, the *IBEX* orbit is outside of Earth's orbit and the gravitational forces of the Sun and Earth add up. In other words, with Earth's gravity the ISN flow is deflected more and the ISN flow detection would be shifted to later times, or larger ecliptic longitude. The additional deflection angle is ($\alpha = 5^\circ$). If *IBEX* could detect the fall signal, then this effect would indeed be beneficial because during this time the *IBEX* orbit is moving out of the magnetosphere.

Figure 5 shows oxygen measurements of the ISN flow during the fall season (Galli et al. 2015). The impact of the magnetosheath and magnetosphere up to orbit 98 (red pixels) is very prominent. The peak of the fall signal was expected to be seen in orbits 97 and 98 (blue arrow). A possible shift of the signal to a later orbit might slightly improve the situation. Such a shift could actually be the cause of a possible signal at one orbit 99 (red arrow). One would also expect a broader, less peaked, distribution. In fact, there are some indications of an elevated signal at spin-angles 120° and 70°. However, the low counting statistics do not allow for a clearer identification of the fall signal.

4.1. Other Possible Gravitational Impacts

The impact of Earth's gravitation potential on the neutral atom measurements in Earth's orbit is most obvious. However, *IBEX* almost reaches the Moon's orbit and neutrals could be deflected by the Moon's gravitation as well. Furthermore, gravitational forces on neutral atoms of large planets, such as Jupiter, could be large enough to generate a measurable change in the *IBEX* signal.

4.1.1. Possible Gravitational Effects of the Moon

Depending on the position of the Moon with respect to *IBEX*, neutral atoms could pass the Moon close enough so that the Moon's gravitation alters their trajectories. Using Equation (4) and the mass of the Moon, we calculated the deflection angle α as a function of the neutral particle speed and the distance the neutral is passing the Moon. The results are shown in Figure 6. During the spring season, the deflection angle is very small ($0^\circ\!.05$), even when the atom passes the Moon at very close distance. During the fall season when the atom velocity is of the order of 20 km s^{-1}, the average deflection angle is still lower than 1°. Also, the possibility that the Moon and *IBEX* are in alignment in the direction of the interstellar flow is relatively small. Furthermore, these time intervals are explicitly eliminated from the ISN flow observations (Möbius et al. 2012; Leonard et al. 2015). Because of this, and the fact that the

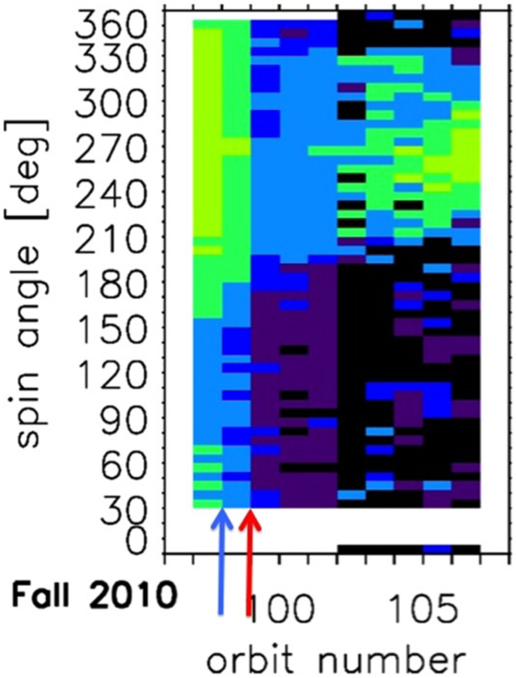

Figure 5. Fall ENA signal during the fall season (2010). The blue arrow indicates the predicted peak location of the fall signal, whereas the red arrow marks the more likely orbit. Modeled after Galli et al. (2015).

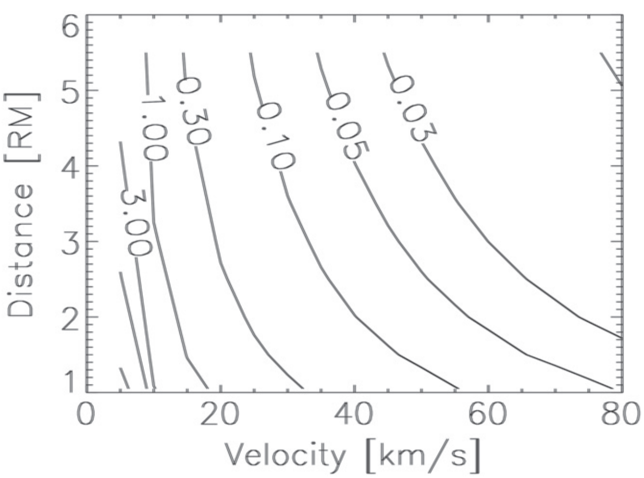

Figure 6. Deflection angle α as a function of ENA velocity and distance r_p (in units of Moon radii) for the Moon. The contours lines are in units of degrees.

deflection is generally very small, the gravitational impact of the Moon on the *IBEX* neutral measurement can be considered negligible.

4.1.2. Possible Gravitational Effects of Jupiter

Jupiter is the largest planet in our solar system with a mass some 317 times the mass of Earth, and thus it has a strong gravitational influence. Its diameter is 11.2 times larger than Earth's. Figure 7 shows the deflection angle as a function of the distance r_P and the neutral velocity. An interstellar neutral passing Jupiter at a distance of 50 Jupiter radii R_J with a speed of 20–32 km s^{-1}, i.e., the typical ISN flow speed, at 5 AU would be deflected by about 10°, which is larger than one pixel of *IBEX*-lo. An area of 50 R_J in radius at a distance of 4 AU from Earth would affect 1/5 of a 6° × 6° *IBEX* pixel.

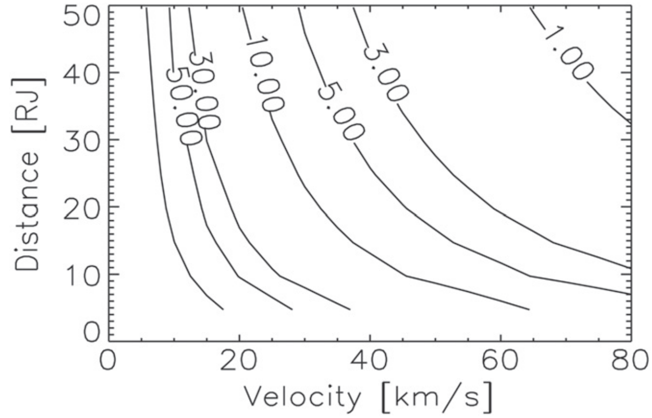

Figure 7. Deflection angle α as a function of ENA velocity and distance r_P (in units of Jupiter radii) for Jupiter. Contour lines are in units of degrees.

Therefore, a Jupiter passage during the ISN flow observation will result in a relatively temporary change of the angular distribution and either an increase or decrease in the intensity, depending on the temperature of the ISN flow or, in other words, a focusing of the ISN flow distribution, as we will investigate in the next section.

4.1.3. The Helium Focusing Cone of Jupiter and the Sun

Using the approach from Feldman et al. (1972), one can determine the helium density variation of the focusing cone of the Sun:

$$n_{\mathrm{He}}(r,\,\delta) = \frac{1}{\delta_c} n_{\mathrm{He}}(\infty) \left(\frac{2b}{r}\right)^{\frac{1}{2}} \exp\left[\frac{-\pi r_{\mathrm{E}}^2 P\left(r_{\mathrm{E}}\right)}{\sqrt{2GMr}}\right], \quad (12)$$

where r is the distance in radial direction to the planet/Sun, δ is the angle from the center of the cone, and $b = GM/\langle V_\infty \rangle^2$:

$$\delta_c = \frac{3}{2}\left(\frac{\pi m \langle V_\infty \rangle^2}{2k_{\mathrm{B}}T}\right)^{-1/2}. \quad (13)$$

In this approach, a parabolic interpolation is used to construct values for n_{He} (r, δ) at arbitrary angles δ:

$$n_{\mathrm{He}}(r,\,\delta) = n_{\mathrm{He}}(r,\,0)(1 - C\delta^2). \quad (14)$$

n_{He} $(r, 0)$ is the helium number density in radial direction. The parameter C is determined by

$$C = \frac{2\pi m \langle V_\infty \rangle^2}{27k_{\mathrm{B}}T}. \quad (15)$$

In these equations k_{B} is the Boltzmann constant and $P(r_{\mathrm{E}})$ is the ionization probability per second at Earth's orbit $r_{\mathrm{E}} = 1$ AU. G is the gravitational constant, M the mass of the Sun (planet), m the mass of the particle, and T its temperature. As one can see in these equations, the ratio of the number density at a certain radial distance $n_{\mathrm{He}}(r, 0)$ and in interstellar space $n_{\mathrm{He}}(\infty)$ depends strongly on the temperature T, the bulk speed at infinity $\langle V_\infty \rangle$, and the $P(r_{\mathrm{E}})$ chosen to be 6.8×10^{-8} s^{-1}. The same equation can be used for Jupiter by turning off/reducing ionization.

Figure 8 shows the ratio $n_{\mathrm{He}}(r, 0)/n_{\mathrm{He}}(\infty)$ for the Sun and Jupiter as a function of the heliospheric distance r from the Sun/Jupiter. The left panel shows the ratio along the center of the cone for the Sun, whereas the right panel shows the

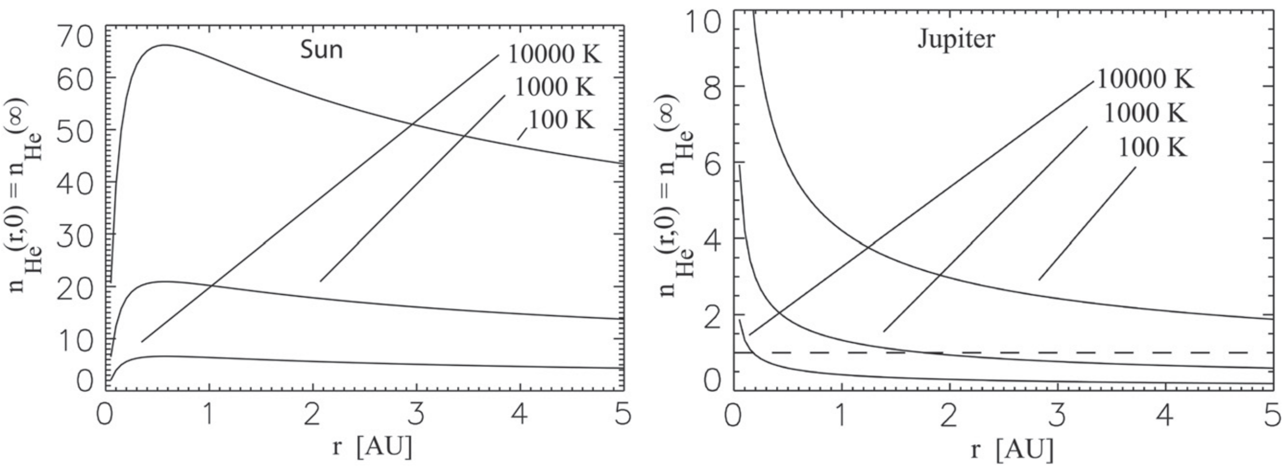

Figure 8. Ratio of $n_{He}(r, 0)/n_{He}(\infty)$ for the Sun (left) and Jupiter (right) as a function of distance and temperature. The dashed line in the right-hand figure shows the unity line ($n_{He}(r, 0)/n_{He}(\infty) = 1$).

situation for Jupiter. As one can see, there is a strong distance and temperature dependence. Due to the Sun's ionization, the ratio starts low and increases quickly with increasing heliospheric distance. It peaks at around 0.5 AU and decreases at larger distances. The temperature dependence of the overall intensity of the ratio could be used as an independent measure of the temperature of helium at infinity.

For Jupiter, the evolution of the ratio as a function of heliospheric distance looks different. Assuming that there is no ionization (a reasonable assumption), the helium ratio is maximal in the close vicinity of Jupiter. Again, depending on the temperature, the helium cone could well exceed 1 AU (which is in agreement with the prediction of Fahr et al. 1976). At some distance, the ratio becomes smaller than one (dashed line), indicating depletion. This happens particularly at high temperatures, but this depletion could be as high as 50%. Considering an average distance from Earth to Jupiter of 4 AU and an ISN temperature of 7500–8000 K (Bzowski et al. 2015; Möbius et al. 2015), it may be worth using *IBEX* to search for a temporary depletion in the ISN flow signal due to the Jovian cone.

IBEX should be able to measure the Helium focusing cone of the Sun. The abundance ratio is well above one (see Figure 8 right side). It peaks inside 1 AU and the peak broadens with increasing temperature. The ratio decreases by a factor of four when the temperature increases from 1000 to 10,000 K. However, the ISN flow atoms have trajectories downwind of the Sun that are too far from tangential to Earth's orbit, and so a larger re-orientation capability is needed than *IBEX* can offer. Therefore, the *IBEX* viewing is not favorable for the cone. In addition, *IBEX* observes the "He Warm Breeze" around the location of the focusing cone (Kubiak et al. 2014). The flux of the ISN flow trajectories that arrive tangential to Earth's orbit in the downwind region is much lower than the Warm Breeze fluxes. For more details on cone observations with pick-up ions, we refer interested readers to Möbius et al. (1995; see also Gloeckler et al. 2004; Drews et al. 2010).

5. CONCLUSION

In this paper, we have investigated the possible impacts of planetary gravitation on *IBEX* ENA measurements as well as on the ISN flow observations and analysis. We investigated possible impacts of Earth's and the Moon's gravitation on the determination of the interstellar parameters during the fall and spring observational seasons. In spring, the impact of Earth's gravitational force is negligible. The maximum deflection is on average 0°.07. Such a small systematic error is included in the overall error estimate (Möbius et al. 2015). During the fall season, Earth's gravitational effects are larger. A larger deflection of the neutral atoms and the ISN flow due to Earth's gravity leads to a significant change of the observed ISN flow peak longitude.

The impact of the Moon's gravitation on the measurements of the interstellar parameters is negligible. First, the Moon is not always in the FOV when *IBEX* measures the interstellar flow. In particular, the Moon viewing time is omitted in the ISN flow analysis. Second, even, if the interstellar neutral atoms would pass the Moon at close distance, the deflection would be still very small. The current sky maps, which have a resolution of 7°, are likely not impacted by Earth's or the Moon's gravitational effects.

Jupiter may have a significant impact on the interstellar neutral trajectories. In the range of 10–50 Jupiter radii and for a speed of ≈20–30 km s^{-1}, the deflection angle is ≈20°–30° and would be registered in different pixels in the detector. In this study, we also have shown that the focusing cone of the Sun, and possibly Jupiter, could be used as an independent measure of the temperature of the interstellar matter.

Future missions measuring neutral (interstellar) particles will have a high angular resolution and take measurements at lower energies, and thus these effects could become more important. For these measurements, one should select satellite positions that are possibly not in Earth's sphere of influence or the sphere of a more massive object, other than the Sun. Therefore, a spacecraft positioned at the L1 Lagrangian point appears to be ideal to avoid potential planetary gravitational effects.

The authors are grateful to the many individuals at the *IBEX* co-investigator institutions who have made this project possible. This work is supported by the Interstellar Boundary Explorer mission as a part of NASA's Explorer Program and partially by NASA SR&T grant NNG06GD55G. A.G. and P.W. thank the Swiss National Science foundation for financial support.

REFERENCES

Bzwoski, M., Kubiak, M. A., Möbius, E., et al. 2012, ApJS, 198, 12
Bzowski, M., Swaczyna, P., Kubiak, M. A., et al. 2015, ApJS, 220, 28
Cornelisse, J. W., Schoeyer, H. F. R., & Wakker, K. F. 1979, Rocket Propulsion and Spaceflight Dynamics (London: Pitman Publishing Limited)
Drews, C., Berger, L., Wimmer-Schweingrumber, R. F., et al. 2010, JGR, 115, A10108
Fahr, H. J., Lay, G., & Blum, P. W. 1976, A&A, 52, 363
Feldman, W. C., Lange, J. J., & Scherb, F. 1972, in Solar Wind, ed. C. P. Sonett, P. J. Coleman & J. M. Wilcox (Washington: Scientific and Technical Information Office, National Aeronautics and Space Administration), 684
Funsten, H. O., Allegrini, F., Bochsler, P., et al. 2009, SSRv, 146, 75
Fuselier, S. A., Bochsler, P., Chomay, D., et al. 2009, SSRv, 146, 117
Galli, A., Wurz, P., Park, J., et al. 2015, ApJS, 220, 30
Gloeckler, G., Moebius, E., Geiss, J., et al. 2004, A&A, 426, 845
Kubiak, M. A., Bzowski, M., Sokol, J. M., et al. 2014, ApJS, 213, 29
Lee, M. A., Kucharek, H., Möbius, E., Xian, W., et al. 2012, ApJS, 198, 13
Leonard, T. W., Möbius, E. M., Bzowski, M., et al. 2015, ApJ, 804, 42
McComas, D. J., Bzowski, M., Fuselier, S. A., et al. 2015, ApJS, 220, 22
McComas, D. J., Alexashov, D., Bzowski, M., et al. 2012, Sci, 336, 1291
McComas, D. J., Allegrini, F., Bochsler, P., et al. 2009, SSRv, 146, 11
McComas, D. J., Carrico, J. P., Hautamaki, B., et al. 2011, SpWea, 9, S11002
Michels, J. G., Raymond, J. C., Bertaux, J. L., et al. 2002, A&A, 568, 385
Möbius, E., Bzowski, M., Frisch, P. C., et al. 2015, ApJS, 220, 24
Möbius, E., Bochsler, P., Bzowski, M., et al. 2012, ApJS, 198, 11
Möbius, E., Hovestadt, D., Klecker, B., et al. 1985, Natur, 318, 426
Möbius, E., Rucinski, D., Hovestadt, D., et al. 1995, A&A, 304, 505
Saul, L., Wurz, P., & Kallenbach, R. 2009, ApJ, 703, 325
Schwadron, N. A., Möbius, E., Kucharek, H., et al. 2013, ApJ, 775, 14
Schwadron, N. A., Möbius, E., Leonard, T. W., et al. 2015, ApJS, 220, 25
van Allen, J. A. 2002, AmJPh, 71, 5
Witte, M., Rosenbauer, H., Keppler, E., et al. 1992, A&AS, 92, 333
Wurz, P., Fuselier, S. A., Möbius, E., et al. 2009, SSRv, 146, 173